Article

Diameter-Selective Solubilization of Single-Walled Carbon Nanotubes by Reversible Cyclic Peptides

Alfonso Ortiz-Acevedo, Hui Xie, Vasiliki Zorbas, William M. Sampson, Alan B. Dalton, Ray H. Baughman, Rockford K. Draper, Inga H. Musselman, and Gregg R. Dieckmann

J. Am. Chem. Soc., **2005**, 127 (26), 9512-9517• DOI: 10.1021/ja050507f • Publication Date (Web): 10 June 2005

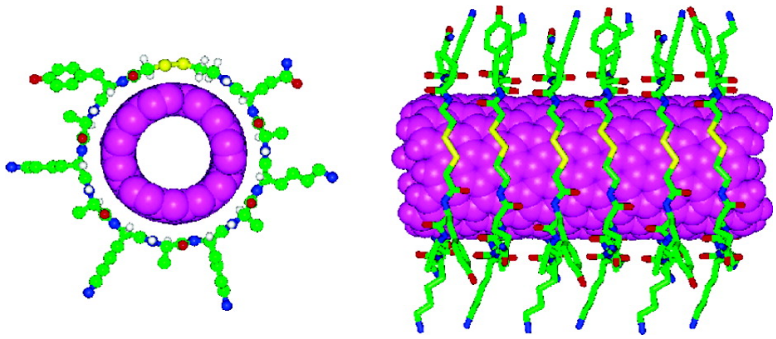

J|A|C|S
ARTICLES
Published on Web 06/10/2005

Diameter-Selective Solubilization of Single-Walled Carbon Nanotubes by Reversible Cyclic Peptides

Alfonso Ortiz-Acevedo,[†] Hui Xie,[†,§] Vasiliki Zorbas,[†] William M. Sampson,[§] Alan B. Dalton,[‡,§] Ray H. Baughman,[†,§] Rockford K. Draper,[†,§,⊥] Inga H. Musselman,[†,§] and Gregg R. Dieckmann*[,†,§]

Contribution from the Department of Chemistry, NanoTech Institute, and Department of Molecular and Cell Biology, The University of Texas at Dallas, 2601 North Floyd Road, Richardson, Texas 75083-0688

Received January 25, 2005; E-mail: dieckgr@utdallas.edu

Abstract: We have utilized reversible cyclic peptides (RCPs)—peptides containing alternating L- and D-amino acids with N- and C-termini derivatized with thiol-containing groups allowing reversible peptide cyclization—to solubilize and noncovalently functionalize carbon single-walled nanotubes (SWNTs) in aqueous solution. Solubilization occurs through wrapping of RCPs around the circumference of a SWNT, followed by the formation of head-to-tail covalent bonds, yielding closed rings on the nanotubes. By controlling the length of the RCPs, we have demonstrated limited diameter-selective solubilization of the SWNTs as revealed by UV/vis/NIR and Raman spectroscopies, as well as atomic force microscopy.

Introduction

Carbon nanotubes (CNTs), which have novel electrical and mechanical properties, have potential biological applications ranging from sensors to tissue supports to artificial muscles.[1] While the literature is extensive on the use of various agents [e.g., surfactants (ref 2 and references therein), polymers (refs 3 and 4 and references therein), polypeptides (refs 5 and 6 and references therein), and nucleic acids (refs 7 and 8)] to disperse CNTs, two major hurdles exist that limit the usefulness of CNTs in many applications: (1) current preparative methods for CNTs generate heterogeneous nanotube mixtures that can vary in length, diameter, and electronic type (semiconducting, semimetallic, and metallic). This heterogeneity ultimately limits the utility of the CNT materials. Recent work on the length,[4,9−13] diameter,[7,8,14] and concomitant length and diameter[15] separation of CNTs, however, has provided important advances in the area of nanotube purification. (2) Unmodified CNTs are very hydrophobic, readily aggregate, and are therefore difficult to interface with biological materials. Detergents such as sodium dodecyl sulfate (SDS) that are commonly used to solubilize CNTs in water would likely disrupt cellular membranes and are incompatible with many biological applications, while covalent modification of CNTs with soluble moieties[16,17] interferes with CNT properties.

To improve CNT solubility in water and biocompatibility, we have developed a family of amphiphilic helical peptides that noncovalently bind and solubilize single-walled carbon nanotubes (SWNTs) in water, yielding unbundled, individual SWNTs.[5,18]Although these helical peptides are excellent solubilization agents, there are two peptide properties that we would like to improve: (1) their affinity for CNTs and (2) the

[†] Department of Chemistry.
[§] NanoTech Institute.
[⊥] Department of Molecular and Cell Biology.
[‡] Present address: Department of Physics, University of Surrey, Guildford GU2 7XH, U.K.

(1) Baughman, R. H.; Zakhidov, A. A.; de Heer, W. A. *Science* **2002**, *297*, 787−792.
(2) Moore, V. C.; Strano, M. S.; Haroz, E. H.; Hauge, R. H.; Smalley, R. E.; Schmidt, J.; Talmon, Y. *Nano Lett*. **2003**, *3*, 1379−1382.
(3) Dalton, A. B.; Blau, W. J.; Chambers, G.; Coleman, J. N.; Henderson, K.; Lefrant, S.; McCarthy, B.; Stephan, C.; Byrne, H. J. *Synth. Met.* **2001**, *121*, 1217−1218.
(4) O'Connell, M. J.; Boul, P.; Ericson, L. M.; Huffman, C.; Wang, Y. H.; Haroz, E.; Kuper, C.; Tour, J.; Ausman, K. D.; Smalley, R. E. *Chem. Phys. Lett*. **2001**, *342*, 265−271.
(5) Dieckmann, G. R.; Dalton, A. B.; Johnson, P. A.; Razal, J.; Chen, J.; Giordano, G. M.; Munoz, E.; Musselman, I. H.; Baughman, R. H.; Draper, R. K. *J. Am. Chem. Soc*. **2003**, *125*, 1770−1777.
(6) Wang, S.; Humphreys, E. S.; Chung, S.-Y.; Delduco, D. F.; Lustig, S. R.; Wang, H.; Parker, K. N.; Rizzo, N. W.; Subramoney, S.; Chiang, Y.-M.; Jagota, A. *Nat. Mater*. **2003**, *2*, 196−200.
(7) Zheng, M.; Jagota, A.; Semke, E. D.; Diner, B. A.; Mclean, R. S.; Lustig, S. R.; Richardson, R. E.; Tassi, N. G. *Nat. Mater*. **2003**, *2*, 338−342.
(8) Zheng, M.; Jagota, A.; Strano, M. S.; Santos, A. P.; Barone, P.; Chou, S. G.; Diner, B. A.; Dresselhaus, M. S.; Mclean, R. S.; Onoa, G. B.; Samsonidze, G. G.; Semke, E. D.; Usrey, M. L.; Walls, D. J. *Science* **2003**, *302*, 1545−1548.
(9) Duesberg, G. S.; Muster, J.; Krstic, V.; Burghard, M.; Roth, S. *Appl. Phys. A* **1998**, *67*, 117−119.
(10) Duesberg, G. S.; Blau, W.; Byrne, H. J.; Muster, J.; Burghard, M.; Roth, S. *Synth. Met*. **1999**, *103*, 2484−2485.
(11) Doorn, S. K.; Fields, R. E., III.; Hu, H.; Hamon, M. A.; Haddon, R. C.; Selegue, J. P.; Majidi, V. *J. Am. Chem. Soc*. **2002**, *124*, 3169−3174.
(12) Farkas, E.; Anderson, M. E.; Chen, Z. H.; Rinzler, A. G. *Chem. Phys. Lett*. **2002**, *363*, 111−116.
(13) Doorn, S. K.; Strano, M. S.; O'Connell, M. J.; Haroz, E. H.; Rialon, K. L.; Hauge, R. H.; Smalley, R. E. *J. Phys. Chem. B* **2003**, *107*, 6063−6069.
(14) Strano, M. S.; Zheng, M.; Jagota, A.; Onoa, G. B.; Heller, D. A.; Barone, P. W.; Usrey, M. L. *Nano Lett*. **2004**, *4*, 543−550.
(15) Heller, D. A.; Mayrhofer, R. M.; Baik, S.; Grinkova, Y. V.; Usrey, M. L.; Strano, M. S. *J. Am. Chem. Soc*. **2004**, *126*, 14567−14573.
(16) Boul, P. J.; Liu, J.; Mickelson, E. T.; Huffman, C. B.; Ericson, L. M.; Chiang, I. W.; Smith, K. A.; Colbert, D. T.; Hauge, R. H.; Magrave, J. L.; Smalley, R. E. *Chem. Phys. Lett*. **1999**, *310*, 367−372.
(17) Chattopadhyay, D.; Galeska, I.; Papadimitrakopoulos, F. *J. Am. Chem. Soc*. **2003**, *125*, 3370−3375.
(18) Zorbas, V.; Ortiz-Acevedo, A.; Dalton, A. B.; Yoshida, M. M.; Dieckmann, G. R.; Draper, R. K.; Baughman, R. H.; Jose-Yacaman, M.; Musselman, I. H. *J. Am. Chem. Soc*. **2004**, *126*, 7222−7227.

10.1021/ja050507f CCC: $30.25

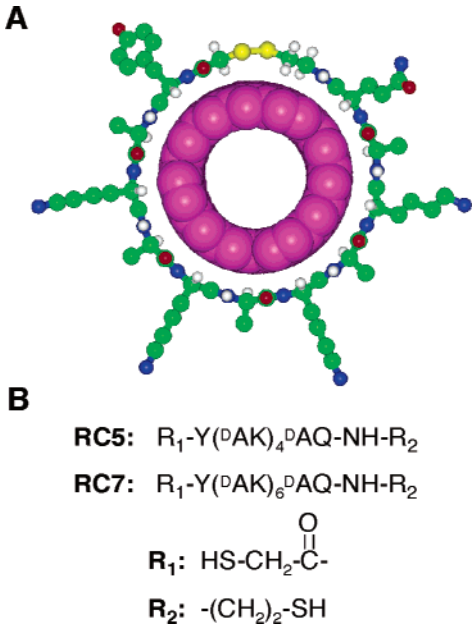

Figure 1. (A) Model (end-on view) of RC5 with a (*11*,*3*) SWNT (C, green; H, white; N, blue; O, red; S, yellow; SWNT, pink). (B) RCP sequences.

selectivity of CNT solubilization, based on either nanotube type or size. Here, we describe a class of peptides that covalently closes around the circumference of CNTs. Encircling CNTs with peptides has two major advantages. One is that the peptides will not dissociate from the CNTs, and therefore they provide extremely stable CNT dispersions. The second is that CNTs can be preferentially solubilized when the nanotube diameter is small enough to be encircled by a given length of peptide, thereby enabling diameter-selective separation of SWNTs.

In this study, we use a novel class of cyclic peptides containing alternating L- and D-amino acids (AAs),[19,20] called reversible cyclic peptides (RCPs),[21] for the diameter-selective solubilization of HiPco SWNTs (Figure 1A). In L-/D-peptides, all side chains reside on one face of the backbone, encouraging a ringlike conformation with the side chains on the ring exterior. In addition, our cyclic peptides have N- and C-termini that are derivatized to contain thiol groups, allowing reversible peptide cyclization through a disulfide bond (Figure 1A). Our results suggest that peptides with different N-to-C-terminal lengths wrap around SWNTs having sufficiently small diameters, promoting selective enrichment of small-diameter CNTs dispersed in solution.

Experimental Section

Peptide Design. Computer-aided modeling utilized the software packages InsightII and Discover (Accelrys Inc., San Diego, CA). The diameter distribution for the HiPco SWNTs used for these studies was previously reported to be 0.7−1.4 nm.[22] To determine the appropriate RCP ring sizes that would selectively encircle CNTs in the 0.7−1.4 nm range, model (*11*,*3*) and (*14*,*5*) SWNT structures with diameters of 1.01 and 1.35 nm, respectively, were created from atomic coordinates obtained from The Nanotube Site (http://www.pa.msu.edu/cmp/csc/nanotube.html). When the van der Waals radii are taken into account, the SWNT diameters are 1.15 and 1.49 nm, respectively. Diameters including van der Waals radii were used to design RCPs of lengths that, when closed into rings, would form pores capable of selectively encircling CNTs of different diameters (Figure 1). The RCPs were generated using backbone dihedral angles reported previously for standard cyclic peptides.[23]

Peptide/CNT Solution Preparation. The peptides RC5 and RC7 were synthesized and purified following previously published methods.[21] Unpurified SWNTs, produced by the method of high-pressure disproportionation of carbon monoxide (HiPco process), were obtained from Carbon Nanotechnologies, Inc., and used without modification. Ultrapure deionized (DI) water was degassed under high vacuum and heated to remove dissolved oxygen that would promote disulfide bond formation in peptide solutions. Degassed DI water was used to prepare all solutions. The concentrations of RCP stock solutions were determined by UV absorbance spectroscopy utilizing the absorbance of the tyrosine residue in each RCP (ϵ = 1420 M^{-1} cm^{-1} at 275 nm). The concentration of free thiol in solution was determined by reacting an aliquot of peptide solution with 5,5′-dithiobis(2-nitrobenzoic acid) (DTNB) in 0.1 M sodium phosphate buffer, pH 8 (Ellman test[24]) and comparing the resulting A_{410} (ϵ = 13 650 M^{-1} cm^{-1}) to a reference solution. The Ellman test was used to determine the free thiol concentration of stock solutions as well as to monitor the oxidation of experimental solutions.

Peptide/SWNT dispersions were prepared by sonicating 1 mL of solution containing HiPco SWNTs (~30 μg) and peptide at a desired concentration. Sonication was performed for specified times using a VWR Scientific Branson Sonifier 250 horn sonicator with a 5 W input energy to the solutions. The dispersions were then centrifuged, and the supernatant was used for all experimental analyses.

UV/Vis/NIR Spectroscopy. RCP/SWNT dispersions were prepared as described above, with the exception that D_2O was used instead of H_2O. Absorption spectra were obtained using a Perkin-Elmer Lamda 900 UV/vis/NIR spectrophotometer and quartz cells having a 1-cm path length. Spectra were collected every nanometer between 200 and 1600 nm.

Raman Spectroscopy. Samples for Raman analysis were prepared as follows. A 100 μM peptide solution was vortexed with 2 equiv of tris(2-carboxyethyl)-phosphine HCl (TCEP; Pierce Biotechnology, Inc., Rockford, IL) for 10 min prior to sonication with HiPco SWNTs. Centrifugation was then carried out in the following sequence: a first spin at 16000*g* for 20 min; the supernatant was placed through a second spin for 30 min at 50000*g*; finally, the supernatant from the second spin was placed through a third spin for 60 min at 100000*g*. The final RCP/SWNT supernatant (~2 μL) was spotted on a SpectRim substrate (Tienta Sciences, Inc., Indianapolis, IN) and allowed to dry in a desiccator overnight prior to Raman analysis. Drying RCP/SWNT dispersions prepared by high-speed centrifugation did not induce the formation of RCP/SWNT bundles on substrates, as demonstrated by AFM of the dried material (Figure 7), similar to previous results with other peptide/SWNT dispersions we have studied.[18] Thus, drying does not make bundles that could influence the Raman spectra. For samples containing SDS, no TCEP was added.

Dispersive Raman spectra were recorded on a Jobin Yvon Horiba high-resolution LabRam Raman microscope system. The laser excitation was provided by a Spectra-Physics model 127 helium−neon laser operating at 633 nm with 20 mW output power (laser in resonance with both metallic and semiconducting CNTs), using a 10× objective lens and a 25-μm slit. The laser power at the sample was ~8 mW and was focused to ~1 μm. Wavenumber calibration was carried out using the 520.5 cm^{-1} line of a silicon wafer. The spectra of peptide/SWNT

(19) Ghadiri, M. R.; Granja, J. R.; Milligan, R. A.; McRee, D. E.; Khazanovich, N. *Nature* **1993**, *366*, 324−327.
(20) Bong, D. T.; Clark, T. D.; Granja, J. R.; Ghadiri, M. R. *Angew. Chem., Int. Ed.* **2001**, *40*, 988−1011.
(21) Ortiz-Acevedo, A.; Dieckmann, G. R. *Tetrahedron Lett.* **2004**, *45*, 6795−6798.
(22) Nikolaev, P.; Bronikowski, M.; Bradley, R.; Rohmund, F.; Colbert, D.; Smith, K.; Smalley, R. E. *Chem. Phys. Lett.* **1999**, *313*, 91−97.
(23) Okamoto, H.; Nakanishi, T.; Nagai, Y.; Kasahara, M.; Takeda, K. *J. Am. Chem. Soc.* **2003**, *125*, 2756−2769.
(24) Ellman, G. L.; Courtney, K. D.; Andres, V., Jr.; Feather-Stone, R. M. *Biochem. Pharmacol.* **1961**, *7*, 88−95.

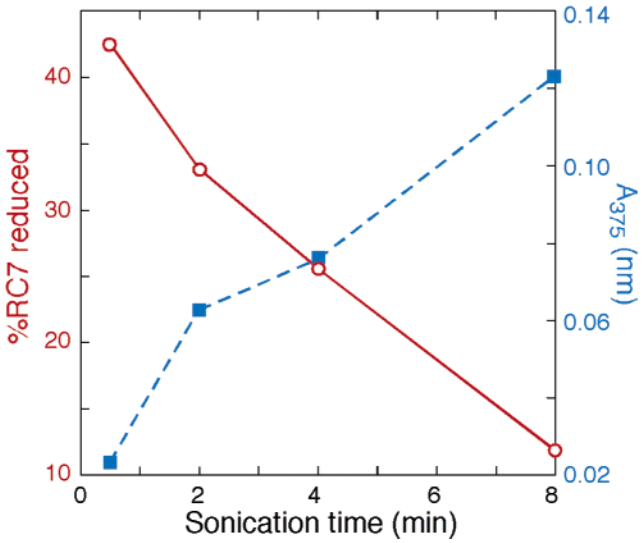

Figure 2. (Left axis, red solid line) Percent reduced RC7 in dispersion as a function of sonication time (measured by Ellman test). (Right axis, blue dotted line) A_{375} for RC7/SWNT dispersion as a function of sonication time.

and SDS/SWNT dispersions were recorded by scanning the 50−2000 cm^{-1} region for a total acquisition time of 8 min.

Atomic Force Microscopy (AFM). Samples were prepared as described in the Raman section. The 100000*g* supernatants were diluted 10-fold with degassed DI water, and 10-μL volumes were dropped onto freshly cleaved muscovite mica (Asheville-Schoonmaker Mica Co.). Samples were placed in a desiccator to dry for 24 h prior to AFM imaging. AFM images (2.0 × 2.0 μm) were acquired in air under ambient conditions using a Digital Instruments, Inc. Nanoscope III Multimode Scanning Probe Microscope operated in the TappingMode with 5.0 N m^{-1} force constant cantilevers and a reduced Z-limit (100 V).[18] The AFM scanner was calibrated using a NanoDevices, Inc. standard consisting of lines with 2-μm pitch and 20-nm height, dimensions similar to those of SWNTs. The height calibration was verified to be 0.3% accurate using hydrofluoric acid etched pits in muscovite mica where 2-nm steps are observed along the long axis and 1-nm steps are observed along the short axis.[25]

Results and Discussion

RCP Design. The appropriate peptide lengths for wrapping SWNTs of different diameters were determined using computer models of RCPs encircling SWNTs. Optimized RCP models suggest that peptides with 11 amino acids (40 backbone atoms) and 15 amino acids (52 backbone atoms) should be sufficient to encircle SWNTs with diameters of 1.15 and 1.49 nm, respectively. An additional seven atoms per peptide come from modifications to the N- and C-termini, yielding the peptides RC5 and RC7 (Figure 1B). The resulting RCPs contain two free thiols, which enable the formation of closed rings upon intramolecular reactions to create disulfide bonds. Both RC5 and RC7 reversibly convert between reduced (linear) and oxidized (cyclized) states, with monomers being the predominant form in a 100 μM peptide solution.[21]

SWNT Solubilization by RCPs. The solubilization of HiPco SWNTs by RC5 and RC7 was studied by sonicating SWNTs in the presence of aqueous RCP solutions and monitoring the SWNT absorbance at 375 nm to determine the amount of dispersed SWNTs. With a reduced (linear) RCP solution, a black

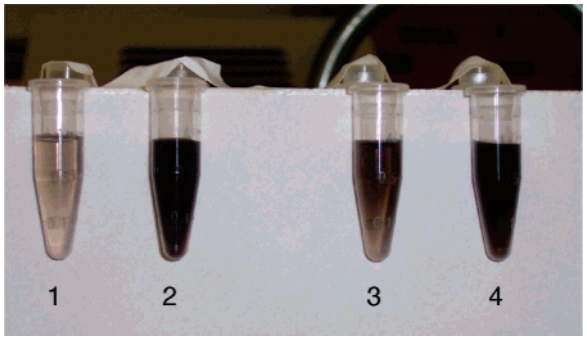

Figure 3. (Tube 1) RC5 initially oxidized (cyclized), sonicated in the presence of SWNTs. (Tube 2) RC5 initially reduced (linear), oxidized in the presence of SWNTs. (Tube 3) RC7 initially oxidized (cyclized), sonicated in the presence of SWNTs. (Tube 4) RC7 initially reduced (linear), oxidized in the presence of SWNTs. For all samples, a 4-min sonication time was used, followed by 16000*g* centrifugation for 10 min.

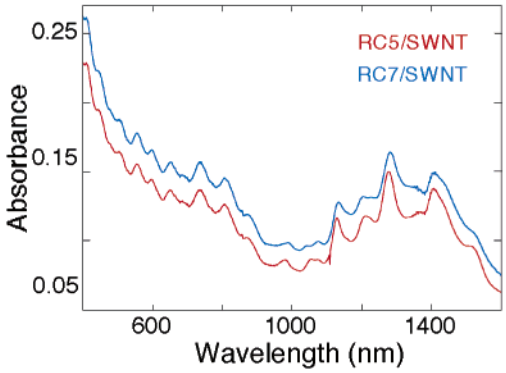

Figure 4. UV/vis/NIR spectra of RC5/SWNT (red, lower spectrum) and RC7/SWNT (blue, upper spectrum) dispersions.

dispersion formed, characteristic of SWNTs in solution, for which A_{375} intensified with increased sonication time (Figure 2). This increase in SWNT concentration with increased sonication time also correlated with a decrease in reduced RCP as measured by the Ellman test (Figure 2); taken together, these results suggest that sonication leads to peptide oxidation (cyclization) with concurrent CNT solubilization.

The amount of SWNTs solubilized also depends on whether the RCP is in the linear (reduced) or cyclized (oxidized) form. When the RCP was initially open, high levels of SWNT solubilization occurred after sonication (Figures 2 and 3); however, solubilization was significantly less efficient with RCPs that were initially in the cyclized state (Figure 3) (the small amount of CNTs that are observed in vials 1 and 3 of Figure 3 are likely due to weak interactions between Lys side chains on each RCP exterior and the CNTs; RC5 (vial 1) has fewer Lys residues than RC7 (vial 3), and thus under the same conditions the longer peptide should yield a slightly higher nanotube solubilization). When control peptides were used that have the same AA sequence as the RCPs but lack terminal thiol groups, less SWNT solubilization occurred (data not shown). In addition, when β-mercaptoethanol was added to an RCP/SWNT dispersion to disrupt RCP disulfides, a majority of the SWNTs precipitated out of solution (data not shown). Furthermore, dilution of RCP/SWNT dispersions with water resulted in minimal SWNT precipitation, suggesting that the RCPs were very tightly bound to SWNTs as predicted if the RCPs were covalently closed around the CNTs. *Taken together, these data strongly suggest that RCPs solubilize and stabilize SWNTs in*

(25) Nagahara, L. A.; Hashimoto, K.; Fujishima, A. *J. Vac. Sci. Technol., B* **1994**, *12*, 1694−1697.

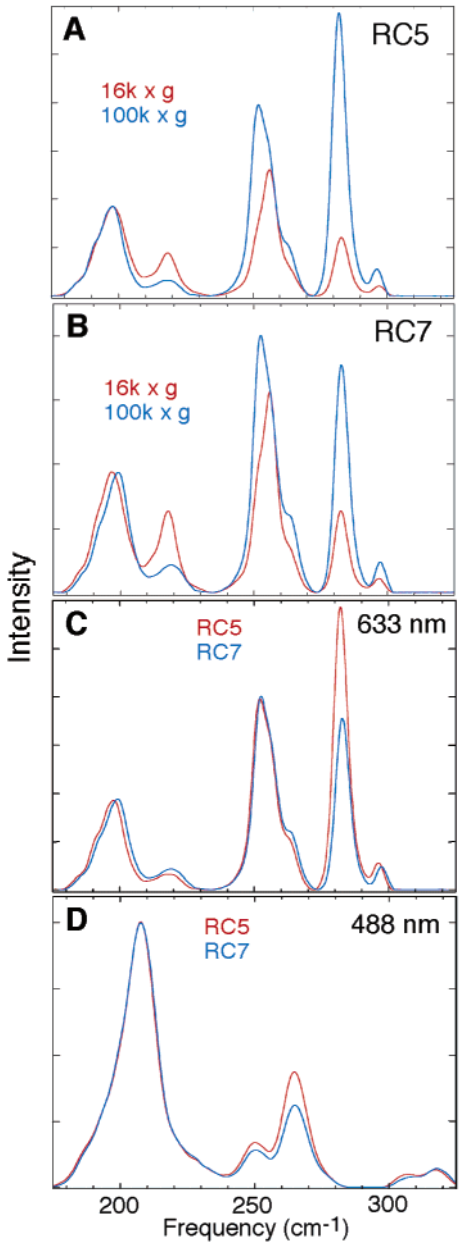

Figure 5. (A and B) Raman RBM regions of RC5/SWNT (A) and RC7/SWNT (B) dispersions (red, 16000*g*, 20 min; blue, 100000*g*, 1 h; 633-nm excitation). (C and D) Comparisons of RBM regions of RC5/SWNT (red) and RC7/SWNT (blue) dispersions excited at 633 (C) and 488 nm (D). All spectra were normalized to the band at ~200 cm^{-1}.

aqueous solution by wrapping around the circumference of the CNTs, forming rings closed by disulfide bonds.

Optical Spectroscopy. The optical absorption spectra of RC5/SWNT and RC7/SWNT dispersions show multiple well-defined peaks from the visible to NIR regions (Figure 4). The peaks represent optical transitions between singularities for a specific type of tube (*n*,*m*) and are evidence that RCPs efficiently debundle HiPco SWNTs. Moreover, for a given peptide concentration, dispersions made with RC7 reproducibly absorb more strongly than those made with RC5. Each RCP, when cyclized, should solubilize all individual SWNTs with diameters smaller than the cyclized peptide's inner pore. Since RC7 is longer, its inner pore when cyclized should be larger and thus

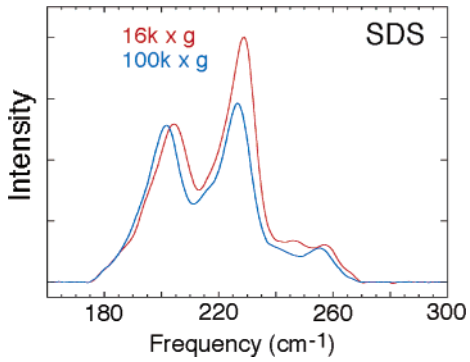

Figure 6. Raman RBM regions of SDS/SWNT dispersion (red, 16000*g*, 20 min; blue, 100000*g*, 1 h; 633-nm excitation). Spectra were normalized to the band at ~200 cm^{-1}.

should solubilize a larger population of SWNTs than cyclized RC5, giving rise to the higher absorbance observed in Figure 4.

Raman Spectroscopy. Diameter selection is further substantiated by Raman spectroscopy of samples centrifuged at different speeds. Centrifugation should remove CNT bundles that are not diameter-selected by RCP wrapping. Therefore, following centrifugation, the diameter distribution of individual SWNTs that are wrapped and maintained in solution by the RCPs can be analyzed. At a constant excitation wavelength (either 633 or 488 nm; 488-nm excitation data not shown), the radial breathing modes (RBMs) of the Raman spectra show intensity changes as a function of centrifugation speed (Figure 5A,B). The same bands were observed in dispersions centrifuged at 16000*g* and 100000*g*; however, the relative intensities depended on the peptide. For the 633-nm excitation, for example, the bands at 252, 282, and 296 cm^{-1} (corresponding to SWNTs with approximate diameters between 0.79 and 0.94 nm[26,27]) are significantly enhanced as the RC5 sample is spun faster, whereas the band at 218 cm^{-1} (~1.1 nm diameter SWNTs) is decreased in intensity (Figure 5A). A similar pattern is observed for the RC7/SWNT dispersion (Figure 5B); however, whereas the 252 and 282 cm^{-1} bands invert their relative intensities for the RC5 sample at faster centrifugation speeds, the relative intensities in the RC7/SWNT dispersion remain similar. Similar patterns are also observed for the RBMs at a 488-nm excitation (data not shown).

The Raman results at different centrifugation speeds suggest a selective enhancement of smaller-diameter SWNTs as the samples are spun faster, with a more significant enhancement occurring for RC5, evidence that smaller-diameter SWNTs are enriched in the RC5 samples. If this effect were simply due to decreasing the concentration of the more dense CNTs in solution at higher speeds (and not to a diameter-selective solubilization), then we would actually expect to see a *decrease* in the RBM features owing to the removal of the smaller-diameter (more dense) CNTs; we observe the opposite trend (the densities associated with RC5/(*11*,*3*)-SWNT and RC7/(*14*,*5*)-SWNT systems were calculated on the basis of our molecular models, including in each calculation all backbone atoms for a single RCP molecule and all carbon atoms in a 10-Å-long slice of a

(26) Bachilo, S. M.; Strano, M. S.; Kittrell, C.; Hauge, R. H.; Smalley, R. E.; Weisman, R. B. *Science* **2002**, *298*, 2361−2366.
(27) Karachevtsev, V. A.; Glamazda, A. Y.; Dettlaff-Weglikowska, U.; Kurnosov, V. S.; Obraztsova, E. D.; Peschanskii, A. V.; Eremenko, V. V.; Roth, S. *Carbon* **2003**, *41*, 1567−1574.

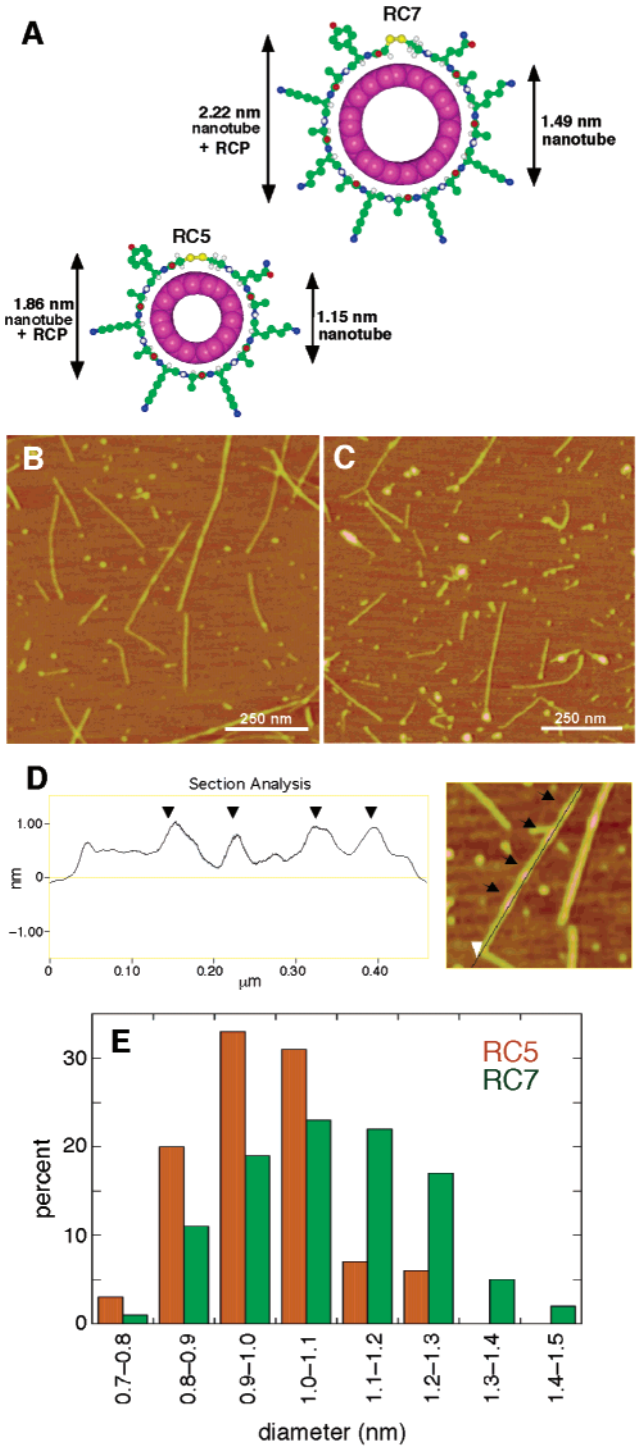

Figure 7. (A) Expected dimensions for RC5/SWNT and RC7/SWNT structures. (B and C) 1.0 × 1.0 μm AFM images of diluted 100000*g* RC5/SWNT (B) and RC7/SWNT (C) dispersions. (D) Left, AFM height profile taken along the length of a single nanotube (right, AFM image, 0.5 × 0.5 μm), showing the differences between the smooth and beaded areas (beaded areas indicated by arrows). (E) Measured diameter distributions (smooth regions) for diluted 100000*g* RC5/SWNT and RC7/SWNT dispersions (n = 100; four 2.0 × 2.0 μm images, two samples for each peptide).

single SWNT; results of the calculations indicate that the smaller-diameter RC5/(*11*,*3*)-SWNT system is ∼6% more dense). For a control system in which diameter selection should not be observed, we prepared SDS-solubilized HiPco CNTs and subjected them to the same centrifugation procedure used for the RCP/SWNT preparations. As can be seen in Figure 6, the RBM signals at higher wavenumbers are repressed in the 100000*g* sample, indicating that larger-diameter CNTs are indeed retained.

Table 1. Statistical Analysis of AFM Height Measurements

	RC5/SWNT		RC7/SWNT	
by nanotube	smooth	bead	smooth	bead
mean (nm)[a]	0.98	1.45	1.12	1.73
SD (nm)	0.13	0.22	0.15	0.30
SD of mean (nm)	0.03	0.06	0.03	0.09
minimum (nm)	0.79	1.41	0.91	1.24
maximum (nm)	1.27	1.79	1.45	2.15
n[b]	17	15	20	11

[a] For each individual nanotube, the mean values for the smooth and beaded regions were calculated. The entries in the table represent the average of the means determined for each nanotube. The height data were also analyzed by separately averaging all smooth and all beaded points for each RCP/SWNT sample (i.e., not calculating a mean for each nanotube), and the results were essentially identical to those reported in this table (not shown). [b] Number of nanotubes per AFM image. The n is different for smooth and beaded regions in a given RCP/SWNT sample because some nanotubes (two for the RC5/SWNT sample; nine for the RC7/SWNT sample) did not have beaded regions present (i.e., were completely smooth).

A similar enhancement is observed at a fixed centrifugation speed (100000*g*) when comparing the RBMs for the RC5/SWNT and RC7/SWNT samples at both 633- and 488-nm excitations. The enhancement is seen for the 282 cm^{-1} band in the RC5 sample at 633 nm (Figure 5C) and for the 265 cm^{-1} band in the RC5 sample at 488 nm (Figure 5D). This demonstrates that the observed changes are not artifacts of a given excitation wavelength.

AFM Height Analysis. Support for diameter selection is also provided by AFM measurements conducted on the RCP/SWNT dispersions. With careful calibration of the scanner, height measurements can be used to accurately determine CNT diameters.[18] RC5 and RC7 are expected to encircle SWNTs with diameters less than or equal to 1.15 and 1.49 nm, respectively. If the peptide backbones of the RCPs are added to the SWNT diameters, the diameters are 1.86 nm (RC5/SWNTs) and 2.22 nm (RC7/SWNTs), respectively (Figure 7A). We have not included peptide side chains in the calculated diameters because the AFM samples are dried; the side chains are expected to collapse onto the surface of the RCP/SWNT structure and not contribute significantly to the measured diameters.

AFM images of the RC5/SWNT and RC7/SWNT dispersions reveal well-dispersed SWNTs (Figure 7B,C). The diameters of the CNTs do not appear completely uniform along their lengths. Rather, the CNTs exhibit smooth regions interrupted by brighter "beaded" areas. These features are possibly associated with bare CNTs (smooth regions) and peptide-wrapped segments (beaded areas). Diameter measurements were obtained at multiple points along each CNT in both the smooth and beaded areas (Figure 7D). For the smooth regions, the diameter distribution for the RC7 sample is shifted significantly to higher diameters compared to that of the RC5 sample (Figure 7E). The diameters range from 0.79 to 1.27 nm for the RC5/SWNT sample versus 0.91 to 1.45 nm for the RC7/SWNT sample (Table 1). A test for unequal variances performed at the 95% confidence level revealed that the average diameters taken along smooth and beaded regions of a CNT can be distinguished between RC5/SWNT and RC7/SWNT samples (Table 1). Importantly, these diameter distributions are both significantly smaller than that

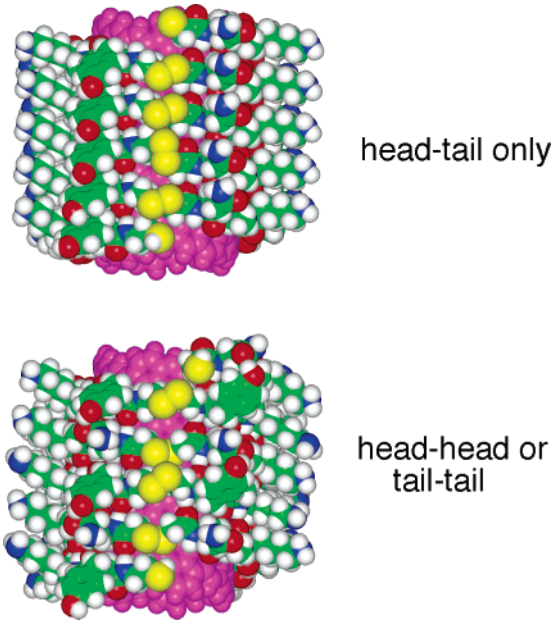

Figure 8. Models showing possible polymerization of RCPs around SWNTs (C, green; H, white; N, blue; O, red; S, yellow; SWNT, pink).

observed for nano-1-wrapped HiPco SWNTs,[18] suggesting that the RCPs solubilize CNTs with smaller diameters.

In the beaded regions, the measured diameters are significantly larger than those in the smooth regions. The measured diameters range from 1.41 to 1.79 nm for the RC5/SWNT sample and from 1.24 to 2.15 nm for the RC7/SWNT sample. These diameters are on average 0.47 and 0.61 nm larger than the smooth regions for RC5 and RC7, respectively, which is close to the expected value of 0.7 nm additional thickness for a single peptide backbone layer surrounding the CNT circumference (Figure 7A). *These AFM measurements strongly support our model for RCP wrapping of SWNTs, displaying diameter distributions consistent with diameter-selective solubilization.*

***Limited* Diameter Selection.** Although RC5 appears to select, on average, smaller-diameter SWNTs than RC7, the selection is not absolute (i.e., RBM bands corresponding to SWNTs larger than 1.0-nm diameter are present in both RCP samples, and a sharp diameter cutoff is not observed in the AFM data). One possible explanation is that the RCPs can polymerize, a known occurrence at high local RCP concentrations (data not shown). Although the peptide concentrations used in this study do not promote significant polymerization in solution, high local concentrations could form if multiple RCPs interacting with the same CNT were in close proximity on the tube surface. Oxidation could then lead to polymerization. Polymers composed of two or more RCP molecules would then be able to wrap SWNTs of various diameters, including those that were too large to be solubilized by cyclized RCP monomers (Figure 8), thus providing a population of SWNTs in the RC5/SWNT dispersion with diameters larger than those allowed by cyclized RCPs.

Conclusions

In conclusion, we have devised a novel way to coat SWNTs with reversible cyclic peptides that covalently close around CNTs through oxidation of thiols incorporated into the peptide backbone. By controlling the length of the RCPs, we have demonstrated limited diameter-selective solubilization of HiPco SWNTs, which may prove useful in SWNT purification. In addition, RCPs covalently closed around SWNTs do not dissociate from the SWNTs unless the disulfide bond is reduced. RCPs thus provide a platform to which other functional groups could be attached without disturbing the covalent structure of SWNTs.

Acknowledgment. Support for this research by the MIRROR Federal Initiative (A.O.-A.), the American Chemical Society Petroleum Research Fund (PRF# 40835-AC3, G.R.D.), the Robert A. Welch Foundation (AT-1326, I.H.M.), the Institute of Biomedical Sciences and Technology (R.K.D. and G.R.D.) and a Department of Homeland Security Fellowship (V.Z.) is gratefully acknowledged.

JA050507F